

**Cell Reports, Volume 26**

**Supplemental Information**

**Structural Basis for Recognition of Ubiquitylated  
Nucleosome by Dot1L Methyltransferase**

**Cathy J. Anderson, Matthew R. Baird, Allen Hsu, Emily H. Barbour, Yuka Koyama, Mario J. Borgnia, and Robert K. McGinty**

**Table S1. Cryo-EM data collection and processing, related to Figure 1.**

	Dot1L -H2BK120ub nucleosome (Classes 3 and 4)	Dot1L -H2BK120ub nucleosome (Class 2A)	Dot1L -H2BK120ub nucleosome (Class 2A masked)
<b>Data collection</b>			
Microscope	FEI Titan Krios	FEI Titan Krios	FEI Titan Krios
Detector	FEI Falcon III	FEI Falcon III	FEI Falcon III
Magnification	75,000	75,000	75,000
Voltage (kV)	300	300	300
Electron exposure ( $e^-/\text{\AA}^2$ )	42	42	42
Defocus range ( $\mu\text{m}$ )	-1.25 to -2.75	-1.25 to -2.75	-1.25 to -2.75
Pixel size ( $\text{\AA}$ )	1.08	1.08	1.08
Symmetry imposed	C1	C1	C1
<b>Data processing</b>			
Initial particle images	408,526	408,526	408,526
Final particle images	101,430	39,558	39,558
Map resolution ( $\text{\AA}$ )	3.5	3.9	7.6
FSC threshold	0.143	0.143	0.143

**Table S2. X-ray crystallography data collection, related to Figure 1.**

	Dot1L-ExoX-H2BK120ub nucleosome
<b>Data collection</b>	
Space group	C2221
Cell dimensions	
$a, b, c$ (Å)	104.97, 200.05, 214.46
$\alpha, \beta, \gamma$ (°)	90.0, 90.0, 90.0
Reflections	29,554
Resolution (Å)	50.00-8.00 (8.14-8.00)
$R_{\text{merge}}$	0.215 (0.765)
$R_{\text{pim}}$	0.068 (0.238)
$I / \sigma I$	19.8 (2.0)
Completeness (%)	97.5 (90.6)
Redundancy	11.7 (9.6)

\*Values in parentheses are for highest-resolution shell.

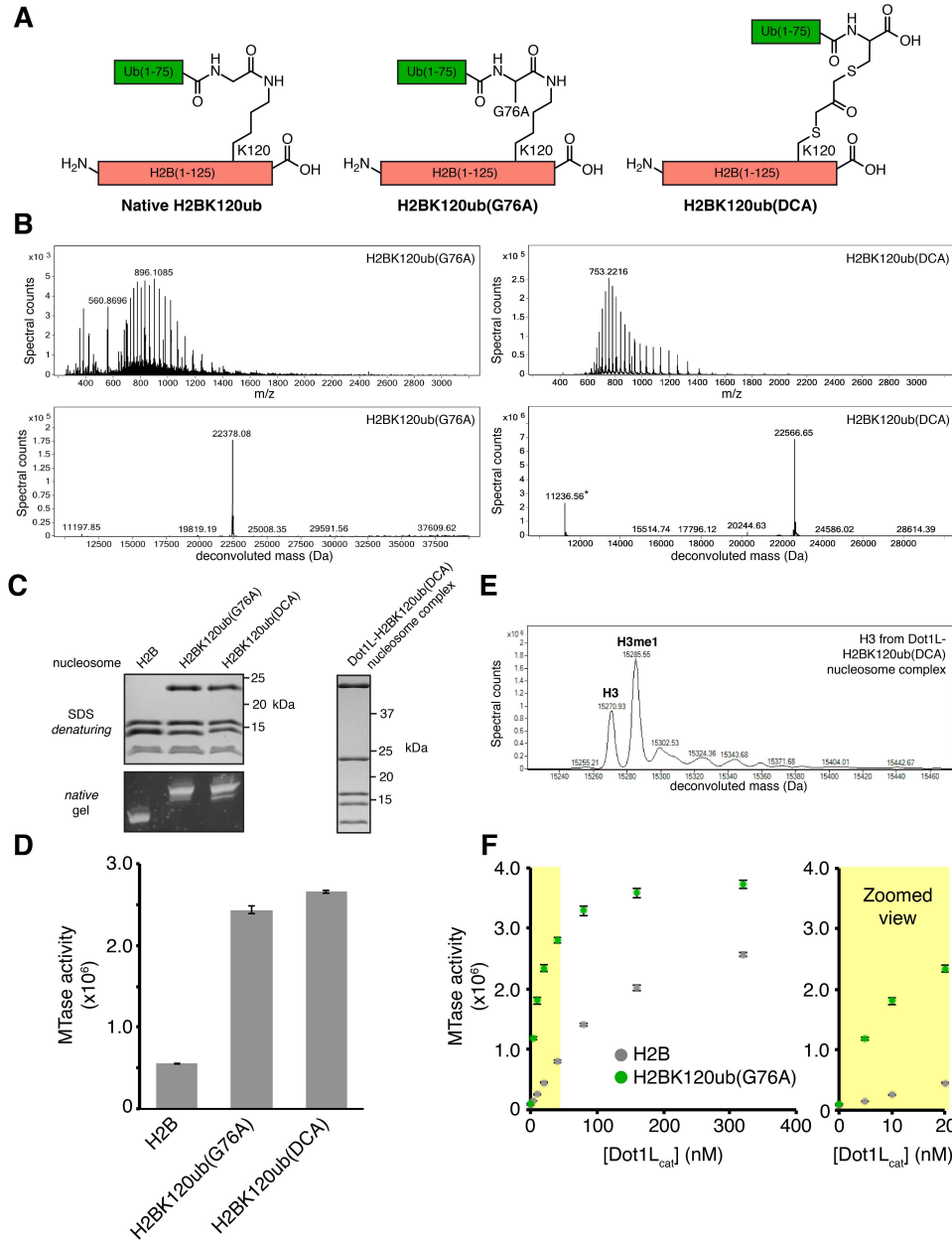


**Figure S1, related to Figure 1. Preparation and characterization of H2BK120ub analogs.** **A**, Scheme showing differences between native, G76A, and DCA-crosslinked linkages at the H2B-ubiquitin junction. **B**, Left, ESI-mass spectrum of semisynthetic H2BK120(Gly76Ala = G76A) (top) and deconvoluted mass spectrum (bottom, expected mass 22,378 Da); Right, equivalent spectra for H2BK120(DCA) from Dot1L-H2BK120(DCA) nucleosome complex (expected mass 22,566 Da; asterisk marks mass of coeluting histone H4). **C**, SDS denaturing and 10% native acrylamide gels of nucleosomes containing unmodified or ubiquitylated H2BK120 (G76A or DCA crosslinked) (left) and of reconstituted Dot1L-H2BK120ub(DCA) complex used for cryo-EM (right). **D**, Quantified methyltransferase assay using nucleosomes reconstituted with indicated unmodified or ubiquitylated H2B. **E**, Deconvoluted ESI-mass spectrum of

histone H3 from Dot1L-H2BK120ub(DCA) nucleosome complex (expected mass unmethylated 15,271 Da, monomethylated 15,285 Da). **F**, Quantified methyltransferase assay with designated Dot1L<sub>cat</sub> concentrations. Zoomed view of indicated region (yellow) at right. Five replicates performed for all assays and means and standard deviations are shown.

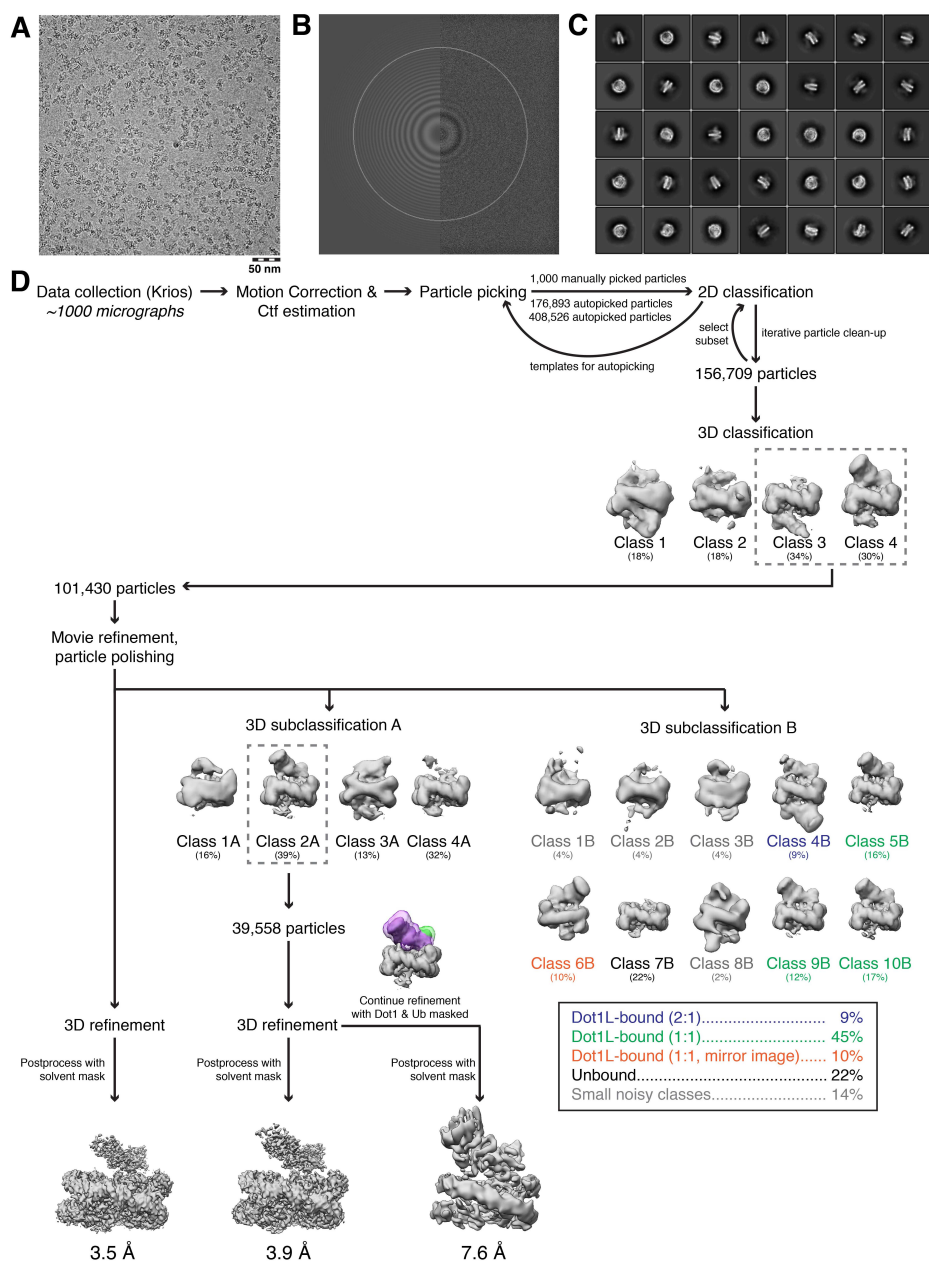


**Figure S2, related to Figure 1. Workflow for cryo-EM data processing.**

Representative **A**, micrograph of complex with 50 nm scale bar, **B**, CTF estimation by GCTF, and **C**, reference-free 2D classifications. **D**, Data analysis scheme showing multiple classification strategies and reconstructed maps discussed in the main text. Classes 3 and 4 of initial 3D classification gave rise to a 3.5 Å map with poorly resolved density for Dot1L and ubiquitin (left). Dot1L and ubiquitin densities were improved by further classification into 4 subclasses leading to a 3.9 Å map from class 2A (middle). The Dot1L and ubiquitin volumes were masked to improve these regions of the map to allow for high confidence docking of high resolution crystal structures into the map.

Finally, finer classification of the particles from the initial classes 3 and 4 into 10 subclasses was used to parse stoichiometric and conformational heterogeneity (right).

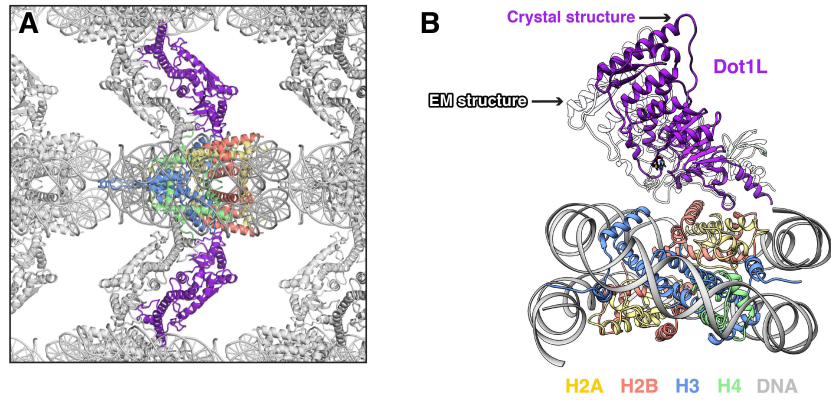


**Figure S3, related to Figure 1. Comparison of X-ray and cryo-EM models of Dot1L-nucleosome complex. A,** Symmetry-related complexes in crystal used for molecular replacement model with one nucleosome and two Dot1Ls colored. Another Dot1L from an adjacent unit cell wedges between Dot1L and the nucleosome to which it is bound on each nucleosome face. **B,** Alignment of cryo-EM and X-ray molecular replacement models using histones for alignment of structures. Dot1L from crystal model (purple) is lifted slightly away from the nucleosome as compared with Dot1L from the cryo-EM structure (white). The nucleosome is only shown for the cryo-EM structure for simplicity.



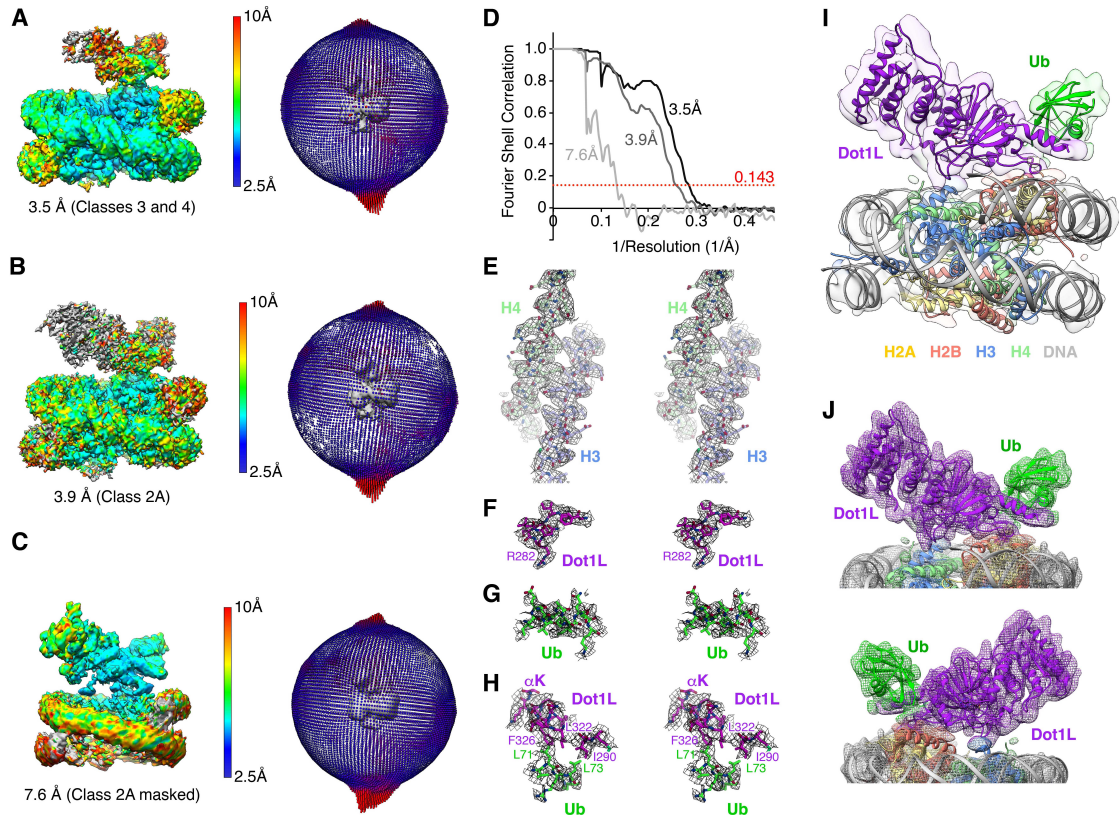


**Figure S4, related to Figure 1. Local and overall resolution of reconstructed maps.** **A**, Reconstructed map (3.5 Å) colored with local resolution (left), and orientational views (right). **B** and **C**, As in **A** for 3.9 Å reconstructed map and 7.6 Å reconstructed map after masking of Dot1L and ubiquitin volumes. **D**, FSC curves for post-processed reconstructions. **E-H**, Stereo views of local EM density maps from 3.9 Å reconstruction of **E**, H3 residues 89-112 and H4 residues 51-76, **F**, the Dot1L nucleosome interaction loop residues 277-284, **G**, ubiquitin residues 23-33, and **H**, Dot1L-ubiquitin interface including Dot1L residues 289-291+322-331 and ubiquitin residues 70-74. Masked .mrc maps in **E-H** contoured at 8 with 2.5 Å carve in PyMOL. **I**, Final model overlaid with 7.6 Å reconstruction from masking of Dot1L and ubiquitin volumes in Class 2A. **J**, Front and back zoomed views of overlay in panel **I**.

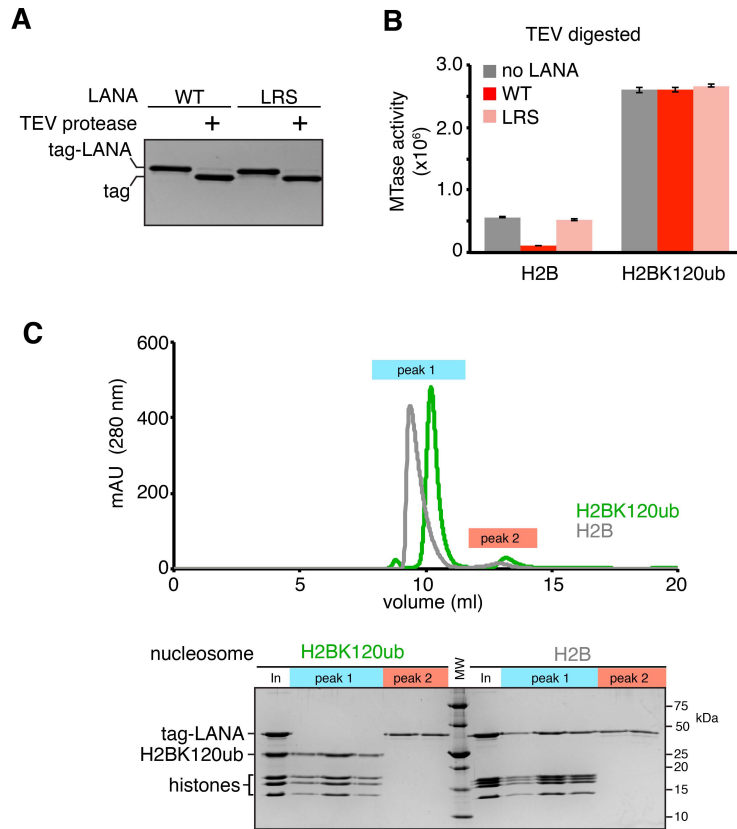


**Figure S5, related to Figure 2. LANA cannot bind H2BK120ub nucleosomes. A,** Denaturing gel showing TEV cleavage of LANA fusions prior to assay in B. Cleaved LANA is not observed on gel due to its small size. **B,** Quantified methyltransferase assay using no LANA or TEV cleaved wild-type or nucleosome binding-deficient (LRS = LRS 8-10 AAA) LANA fusion proteins on unmodified and H2BK120ub nucleosomes. **C,** Overlaid gel filtration chromatograms of reconstituted LANA-unmodified nucleosome complex and failed LANA-H2BK120ub nucleosome reconstitution (top). Peak 1 contains nucleosome or nucleosome-LANA complex and peak 2 contains free LANA fusion protein. Gel of representative fractions from each peak is shown (bottom). Five replicates performed for all assays and means and standard deviations are shown. In = Input.

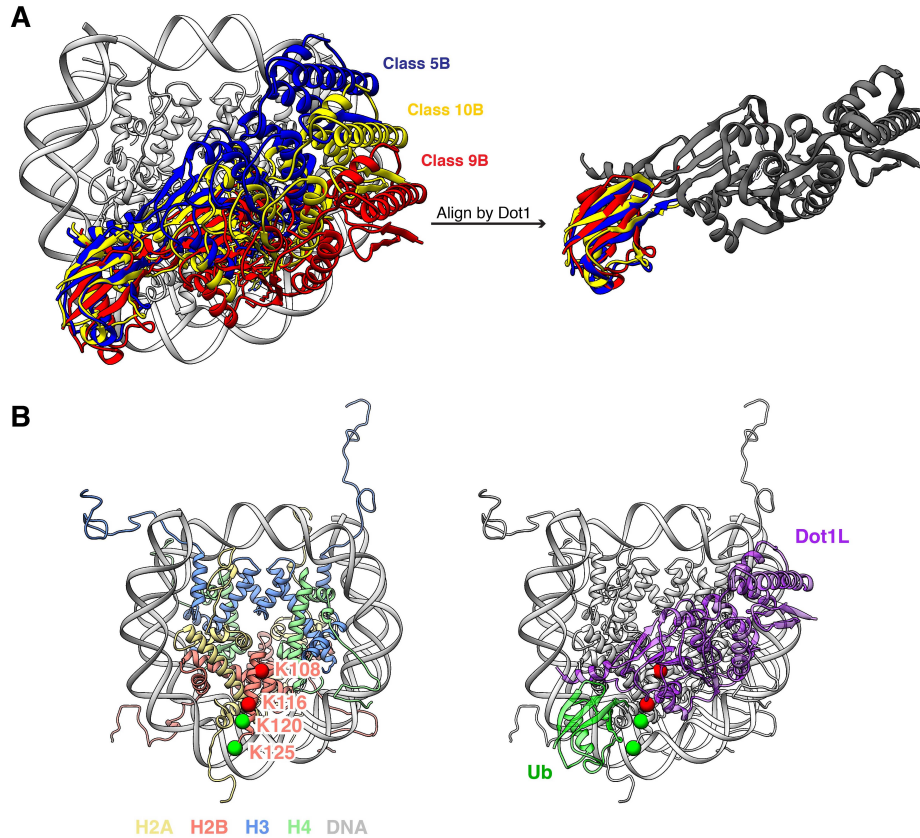


**Figure S6, related to Figure 3. Analysis of ubiquitin conformational heterogeneity and attachment site relative to Dot1L.** **A**, Overlay of docked structures for subclasses 5B, 9B, and 10B with Dot1L and ubiquitin colored (left). Alignment of Dot1L in these classes show that the ubiquitin maintains a similar orientation relative to Dot1L (right). **B**, Left, top view of nucleosome (PDBID 1KX5) with positions of C $\alpha$  atoms from H2BK108, K116, K120, and K125 indicated. Dot1L is activated by ubiquitin attachment at green but not red sites. 1KX5 was used because H2BK125 is not observed in poised Dot1L-bound structure. Right, same view with Dot1L and ubiquitin from cryo-EM structure overlaid and displayed with transparency to allow visualization of underlying histone positions.